

Two-dimensional germanium islands with Dirac signature on Ag₂Ge surface alloy

Jiaqi Deng¹, Gulnigar Ablat¹, Yumu Yang¹, Xiaoshuai Fu¹, Qilong Wu¹, Ping Li^{2,*}, Li Zhang¹, Ali Safaei³, Lijie Zhang^{1,*}  and Zhihui Qin¹

¹ Key Laboratory for Micro/Nano Optoelectronic Devices of Ministry of Education & Hunan Provincial Key Laboratory of Low-Dimensional Structural Physics and Devices, School of Physics and Electronics, Hunan University, Changsha, 410082, People's Republic of China

² Center for Spintronics and Quantum Systems, State Key Laboratory for Mechanical Behavior of Materials, School of Materials Science and Engineering, Xi'an Jiaotong University, Xi'an, Shaanxi, 710049, People's Republic of China

³ Metallurgy and Materials Engineering Department, University of Gonabad, Khorasan Razavi, Iran

E-mail: pli@xjtu.edu.cn and lijiezhang@hnu.edu.cn

Received 17 December 2020, revised 6 February 2021

Accepted for publication 17 February 2021


Published 5 May 2021



Abstract

Two-dimensional (2D) Dirac materials have attracted intense research efforts due to their promise for applications ranging from field-effect transistors and low-power electronics to fault-tolerant quantum computation. One key challenge is to fabricate 2D Dirac materials hosting Dirac electrons. Here, monolayer germanene is successfully fabricated on a Ag₂Ge surface alloy. Scanning tunneling spectroscopy measurements revealed a linear energy dispersion relation. The latter was supported by density functional theory calculations. These results demonstrate that monolayer germanene can be realistically fabricated on a Ag₂Ge surface alloy. The finding opens the door to exploration and study of 2D Dirac material physics and device applications.

Keywords: germanene, Ag₂Ge, 2D Dirac material, scanning tunneling microscopy, scanning tunneling spectroscopy

 Supplementary material for this article is available [online](#)

(Some figures may appear in colour only in the online journal)

1. Introduction

Two-dimensional (2D) materials have attracted a lot of attention due to their exotic properties and appealing applications since the successful isolation of graphene [1, 2]. Germanene, the germanium analog of graphene, shares many properties with graphene [3, 4]. The electrons in germanene are predicted to host Dirac properties such as linear dispersing energy bands near the *K* points of the Brillouin zone [5, 6]. Furthermore, germanene has a much larger spin-orbit gap than graphene [7], making it suitable for different applications. In order to

exploit the unique properties of 2D materials for technological applications, it is of utmost importance to master the art of controllable growth of such materials with clearly understood growth mechanism and parameters. Despite many previous attempts on different substrates [8–14], its growth and subsequent characterization remain inconclusive.

Theoretical calculation demonstrated that germanene can adhere to Ag(111) via electrostatic interactions [15]. However, Dávila *et al* [9] proposed that germanene will not be grown on Ag(111) due to the lattice mismatch and the possibility of forming Ag₂Ge surface alloy [16]. Moreover, prior to the emergence of germanene, germanium had also been found to form a Ag₂Ge surface alloy on Ag(111) surface when 1/3

* Authors to whom any correspondence should be addressed.

monolayer Ge deposited on the substrate [16, 17]. Recently, Lin *et al* found two phases of germanene on Ag(111) substrate, the so-called striped phase and quasi-freestanding phase [18], attributed to the commensurability of the adlayer with the substrate. Zhuang *et al* reported on the successful growth of germanene on a thin film of germanium that was deposited on an Ag(111) substrate [19], though earlier reports had claimed that germanium deposition on Ag(111) leads to the formation of only a crystalline film rather than anything else [20]. Quite recently, Zhang *et al* reported the growth of germanium on Ag(111) at a specific temperature range of 380–430 K. The authors extrapolated the obtained disorder hexagonal structure after higher amounts Ge deposition contains Ag as well [21]. However, it still lacks direct evidence since the scanning tunneling microscopy (STM) do not have an element-specific capability. Furthermore, electronic properties measurement of the formed adlayer, for instance scanning tunneling spectroscopy data, were lacking in their study. Overall, the growth of germanene on Ag(111) is still unclear. A scrutinization of the growth of germanium on Ag(111) will be helpful in understanding the formation of germanene.

In this work, we employ STM and first-principle density functional theory (DFT) calculations to investigate the deposition and growth of germanium on Ag(111) surface. At a low deposition flux, irregular-shaped 2D islands of germanium are formed on the substrate. Upon increasing the deposition flux, the irregular-shaped islands convert to compact 2D islands. These germanium islands are grown in 2D mode, and their differential conductivity is found to be V-shaped around the Fermi level, which is a hallmark of germanene, a 2D Dirac material [22, 23]. These 2D germanium islands have always been found to grow exclusively on the previously formed domain of a different phase that we believe is the Ag_2Ge surface alloy. Meanwhile, our DFT calculations show that germanene on a bilayer Ag_2Ge surface alloys with a V-shaped profile of density of states near the Fermi level. Therefore, our findings suggest that we have successfully synthesized germanene on a bilayer of Ag_2Ge surface alloy supported by Ag(111) surface. The present work suggests that the Ag_2Ge surface alloy could be the precursor phase for the formation of germanene.

2. Methods

The experiments were carried out at a home-made ultrahigh vacuum (UHV) chamber ($<1.0 \times 10^{-10}$ millibar) equipped with an STM (Unisoku Co., Ltd.). The substrate was a single-crystal Ag(111), and was cleaned by several cycles of Ar^+ ion sputtering (1 keV) with subsequent annealing in UHV. The deposition of germanium was done by heating high-purity Ge seeds (Alfa Aesar Puratronic 99.9999%) in a commercial Knudsen cell mounted on the UHV chamber. Subsequently, we annealed the sample mildly (around 450 K) for 5 minutes. The deposition flux was roughly calibrated by the coverage on the substrate. All the STM measurements were made at room temperature. A standard lock-in amplifier was employed for the differential conductivity (dI/dV) measurements by a modulating signal of 50 mV and 773 Hz. The dI/dV spectra shown in this work are all point measurements.

Our DFT-based first-principles calculations were implemented using the *Vienna ab initio simulation package* [24, 25]. The electron exchange correlation functional was described by the generalized gradient approximation of the Perdew–Burke–Ernzerhof function [26]. The plane-wave basis set with a kinetic energy cutoff of 400 eV was used. The geometry optimization for obtaining the final structures was based on minimizing the remaining Hellmann–Feynman forces to less than $0.01 \text{ eV } \text{\AA}^{-1}$. $9 \times 9 \times 1$ ($12 \times 12 \times 1$) k -meshes were adopted for the structural optimization and the self-consistent calculations. To avoid unnecessary interactions between the monolayer, the vacuum layer was set to 20 \AA .

3. Results and discussion

An atomically clean Ag(111) substrate is required for the deposition of germanium. Figure 1(a) shows a large-scale STM image of a clean Ag(111) substrate. The measured step height of 0.22 nm agrees well with the inter-planar distance of (111) planes of a face-centered cubic (fcc) crystal with the lattice constant of 0.289 nm [27]. The empty-state STM image in figure 1(b) reveals that the periodicity of the surface texture is about 0.28 nm which fits quite well with the lattice constant of the Ag(111)-(1 \times 1) structure. The corresponding fast Fourier transform (FFT) depicted in the inset image of figure 1(b) agrees well with the high-resolution STM image.

Figure 1(c) shows the morphology of the surface with the deposition of germanium for 15 min with the rate of about $0.022 \text{ ML min}^{-1}$ and an annealing subsequently. Irregular-shaped domains with two distinct contrasts are visible in the figure. It has been reported that the substitution of very small amount of Ge and Ag to form dark spots due to the smaller radius of Ge than Ag [17]. Similarly, the dark area here are the enlarged spots with increasing amount of substitution of Ge with top layer Ag. And, these dark areas act as nucleation centers for the growth of 2D Ge islands [28]. It explains why these germanium islands are all located on top of the dark region. The branches of the irregular-shaped islands are of monoatomic height with constant thickness, which is supported by the height-profile shown in the inset of figure 1(c). Figure 1(d) shows a zoom-in STM image of irregular Ge structure revealing that germanium on Ag(111) at low coverage grows in the form of 2D instead of three-dimensional (3D) islands. However, these irregular Ge clusters are not likely crystalline structure hindering the atomic resolution image resolved by STM.

To further study the growth of germanium on Ag(111), we increased the deposition flux to $0.062 \text{ ML min}^{-1}$, i.e. to about three times larger than that of the previous deposition, keeping all other parameters unchanged. The result of this deposition has been given in figure 2(a). Three different contrast levels are visible in the figure: bright domains, less-bright areas, and dark domains. Figure 2(b) gives two different periodicities of $0.48 \pm 0.02 \text{ nm}$ and $0.28 \pm 0.02 \text{ nm}$ which agree with the lattice constants of Ag_2Ge surface alloy [17] and bare Ag(111) surface, respectively. Furthermore, the dI/dV spectrum on the

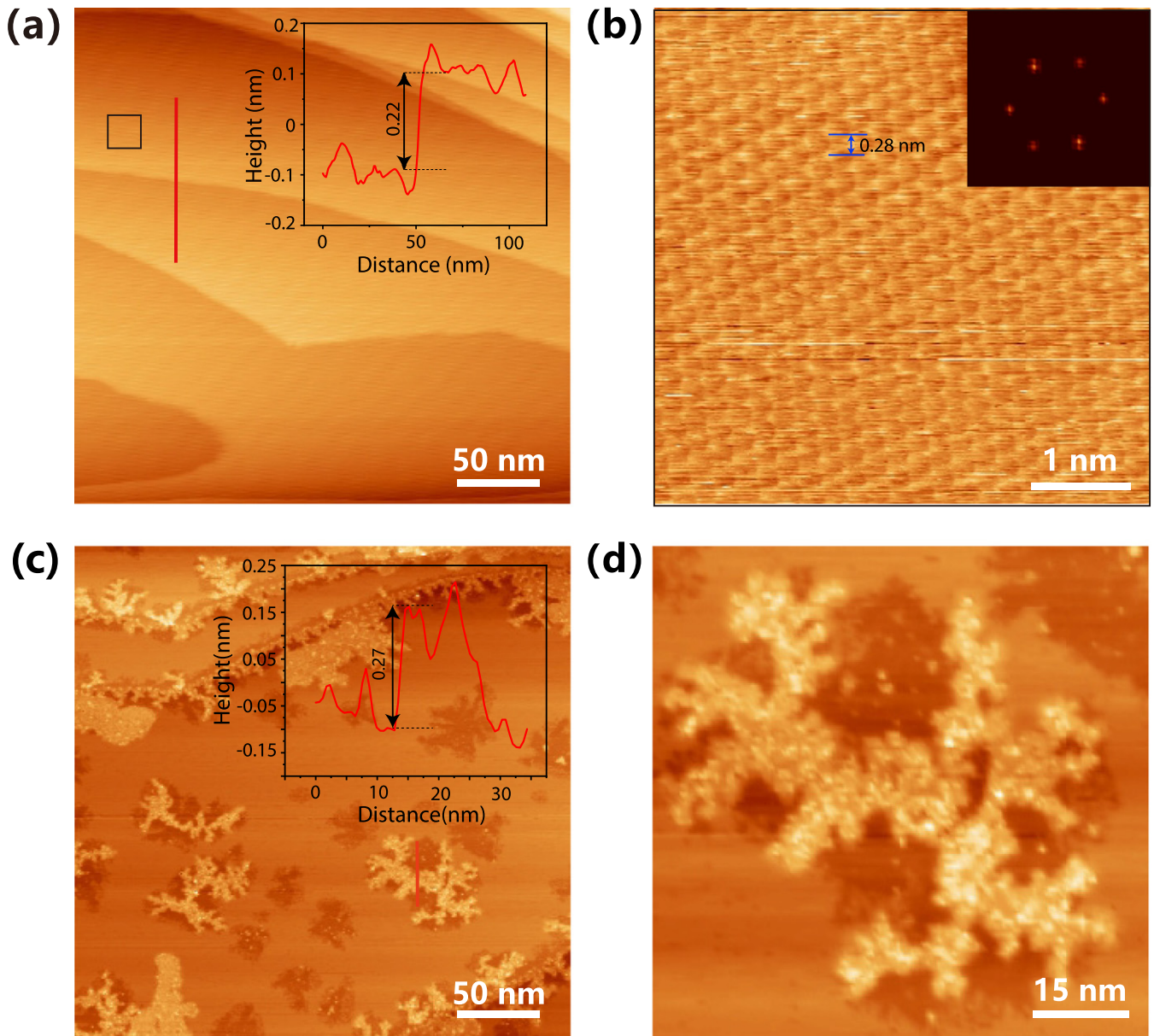


Figure 1. (a) Large-scale STM image of clean Ag(111) surface. The sample bias and setpoint are 1 V, 100 pA. (b) Zoom-in atomic resolution STM image (200 mV, 1.2 nA) with an inset FFT. (c) Large-scale STM images of Ge-deposited Ag(111). The deposition flux was 0.02ML min^{-1} . The bright irregular islands are 2D islands of germanium, and the dark irregular islands are Ag_2Ge surface alloy domains. The less-bright areas are the remaining parts of the pristine Ag(111) surface. The were -1.7 V and 10 pA. The inset shows the height profile of a germanium irregular domain. (d) Zoom-in STM image of the Ge irregular island (-1.7 V, 10 pA).

less-bright areas shown in the figure 2(c) exhibits a typical feature that is consistent with the known surface state onset below the Fermi level of the Ag(111) surface [29, 30]. The energy shift of the typical peak of the dI/dV curve is about 50 meV, due to thermal drift [30]. Figure 2(d) gives the dI/dV spectrum of the dark-contrast domains of figure 2(a)—the metallic character is clearly seen in this spectrum. Therefore, we identify the dark fractal domains in figure 2(a) as the Ag_2Ge surface alloy, and the less-bright areas of figure 2(a) as the remaining parts of the pristine Ag(111) surface. Later on, we provide more evidence that the brightest areas of figure 2(a) are germanium islands.

It should be noted here that the bright and dark domains in figure 2(a) are compact as opposed to the corresponding irregular domains found in figure 1(c). This shape transition of the Ge domains and the Ag_2Ge domains—the brightest and dark domains, respectively—in figure 2(a) in comparison to figure 1(c) might indicate that the growth of the 2D islands of Ge on Ag(111) is a reaction-limited aggregation process rather than a diffusion-limited aggregation [31]. Such 2D islands transition was first observed for the growth of Ge islands on a Pb-covered Ag(111) substrate [31]. One may think that the Ag_2Ge surface alloy acts as a surfactant for the growth of 2D islands of germanium.

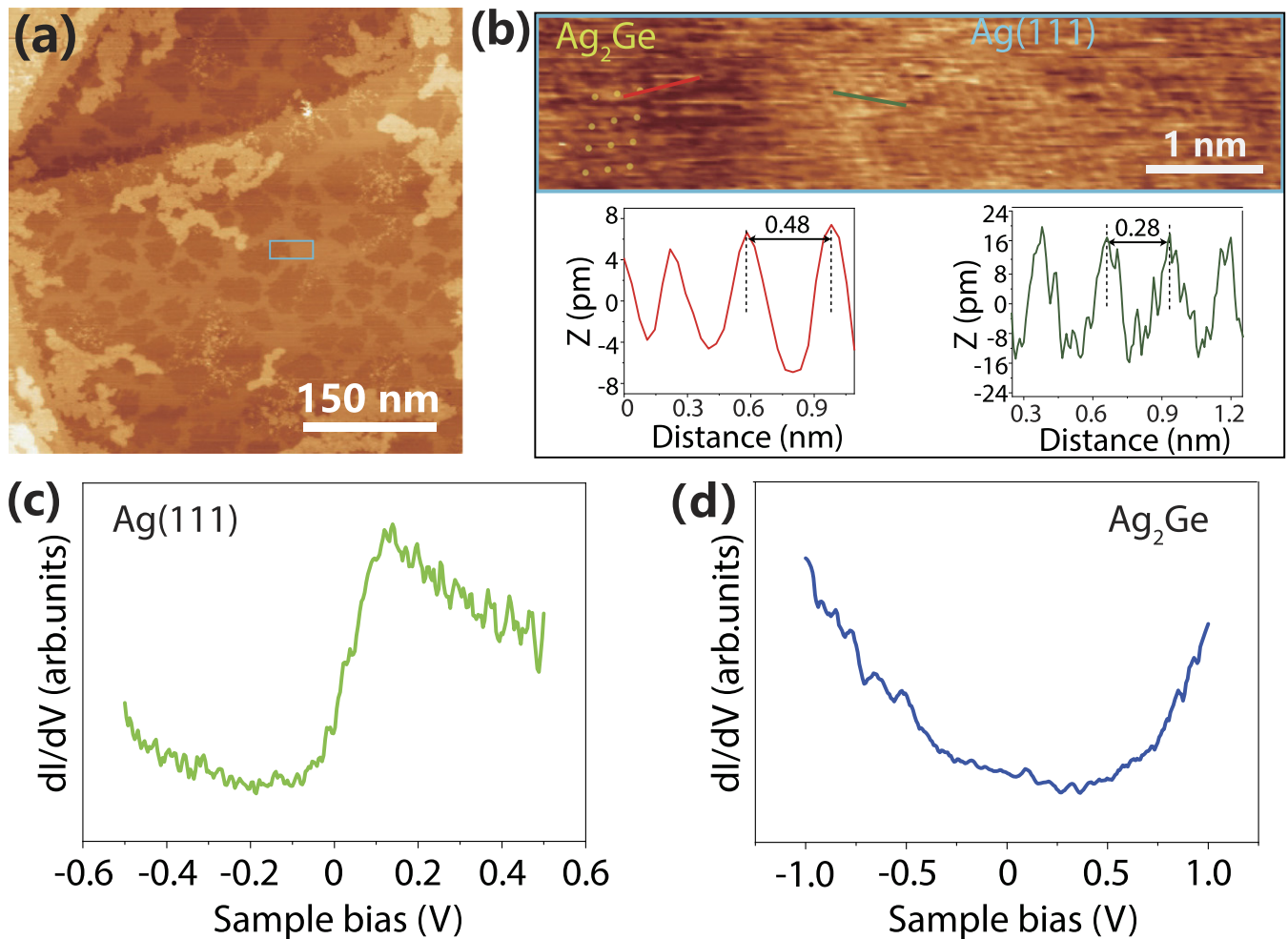


Figure 2. (a) Large-scale STM images of Ge-deposited Ag(111) surface. The deposition flux was $0.062 \text{ ML min}^{-1}$. The set points are 100 pA and 1 V. The brightest areas are 2D irregular islands made of germanium. The less-bright areas are parts of the bare Ag(111) surface that are left untouched by the deposition; and the dark-contrast areas are the irregular islands of Ag_2Ge surface alloy formed upon deposition of $1/3$ of monolayer of Ge at room temperature. (b) High-resolution STM image of the Ag_2Ge and Ag(111) structures (800 pA, -200 mV). The Bottom-left panel and -right panels show the line profiles within the Ag_2Ge and Ag(111) phases, respectively. (c) The dI/dV versus sample-bias spectrum of the Ag(111) phase, and (d) that of the Ag_2Ge phase.

A large-scale image of the brightest areas of figure 2(a) has been given in figure 3(a). The apparent height of the bright-contrast island shown in figure 3(a) is about 0.25 nm (see the inset of figure 3(a)), consistent with the height of a single-layer germanium. Carefully inspecting the STM images, we observe that these 2D islands of bright contrast are indeed always on top of the dark domains that we have already identified as the Ag_2Ge surface alloy; that is, these bright 2D domains always grow on top of the domains of the Ag_2Ge surface alloy—the dark domains—rather than directly on the pristine Ag(111) substrate. Upon further deposition of germanium, those germanium atoms that had taken the positions of silver atoms at the top surface layer can act as nucleation centers for the growth of 2D islands of germanium—similar to what has been observed for the growth of antimonene on SbAg_2 surface alloy covered Ag(111) [32], and stanene/ Ag_2Sn on Ag(111) [33]. It explains why all these germanium islands are located on top of the dark regions, i.e. on the Ag_2Ge phase. Unfortunately,

atomic resolution honeycomb structure of germanene has not achieved here. The dI/dV of these bright domains, which is proportional to their local density of states, exhibits a well-defined V-shape (see figure 3(b)). Such a V-shaped curve of density of states is one of the hallmarks of a 2D Dirac system, that is, revealing a signature of linear energy dispersion relation [22, 23]. It also excludes the possibility that we are dealing with the growth of regular or amorphous germanium. The residual conductivity at the zero bias in figure 3(b) reflects the metallic character of the material that is beneath the germanene islands. It has been calculated that the Dirac properties of germanene can be preserved on Ag although slightly hybridized [34]. The energy range of this V-shaped curve of density of states is about 0.2 eV, which is in agreement with the prediction of germanene in previous theoretical calculation [5]. Interestingly, Zhuang *et al* [19] found that germanene terminated on top of Ge(111) nanosheets on an Ag(111) substrate, which is, however, different from our case.

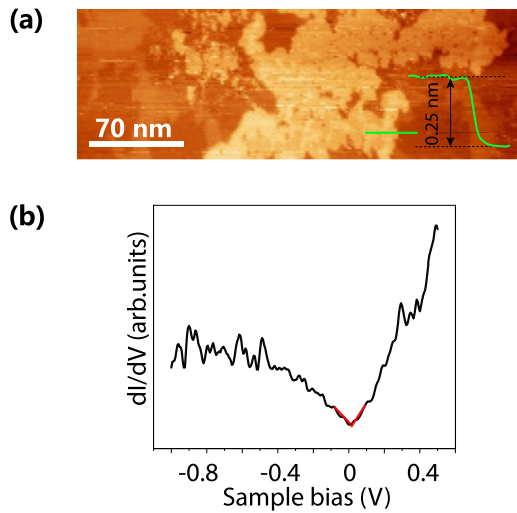


Figure 3. (a) A large-scale STM image of figure 2(a) sample (100 pA, 1 V). The bright contrast is for germanene islands; the less-bright contrast is for the pristine Ag(111) surface. And the dark contrast is for the Ag_2Ge surface alloy. The inset height profile of the germanene island through the green line segment in (a). (b) The differential conductivity record on the germanene island.

We observed that the deposition rate could substantially change the nucleation of germanium clusters. At a low deposition rate, Ge atoms can meet each other slowly; they then react with the surfactant Ag_2Ge to form the Ge irregular islands. At a deposition rate three times higher than the previous one, the deposited Ge atoms are more mobile to meet and overcome the nucleation barrier to form crystalline growth mode. In a recent study, Yuhara *et al* [35] synthesized germanene by segregating through Ag thin films, which means the Ge–Ge interaction is stronger than Ge–Ag bonding, and boosts the formation of germanene layer. A follow-up work has used a similar recipe to segregate germanene between 2D material covered Ag(111) surface [36]. It is worth mention that Zhang *et al* performed the deposition of Ge on Ag(111) and found a hexagonal structure of the adlayer with a lattice constant of $4.3 \pm 0.2 \text{ \AA}$ [21], which is, actually, quite close to the predicted freestanding germanene of 3.97 \AA [5]. Furthermore, the lattice constants of germanene will be slightly stretched if the buckling is lower than the freestanding condition, which had been reported in germanene/ Ge_2Pt system [8, 23].

In order to further confirm our results, we perform first-principle DFT calculations on four different structures of germanene on monolayer, bilayer, and trilayer Ag_2Ge substrate. We have found that only the germanene/bilayer- Ag_2Ge bridge-Ag–Ag structure gives rise to a well-defined V-shaped profile of density of states in the vicinity of the Fermi level (see figure 4(a)), which is in good agreement with the experimental findings. Figures 4(b) and (c) show, respectively, the top- and side-views of the structure. In other words, the germanene-on-monolayer- Ag_2Ge and the germanene-on-trilayer- Ag_2Ge systems never show a V-shaped curve of density of states near their Fermi levels (see figure S1 (<https://stacks.iop.org/JPCM/33/225001/mmedia>) in supplementary material). To understand this, we need to first analyze

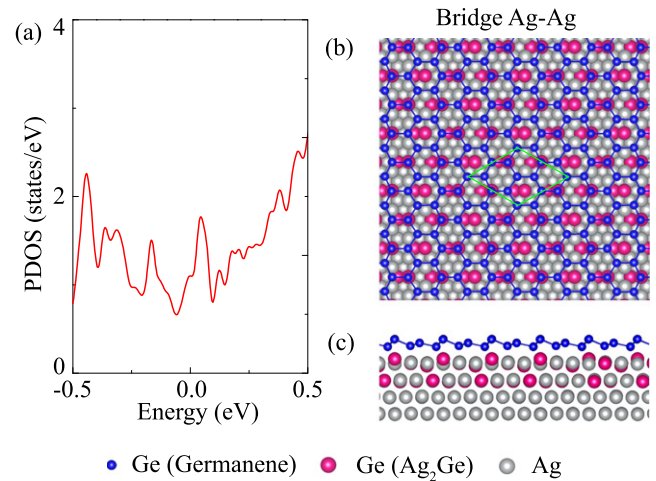


Figure 4. Schematic atomic structure and PDOS calculated within the DFT for bridge-Ag–Ag structure of germanene on bilayer Ag_2Ge substrate. (a) The PDOS of germanene. (b) Top-view structure (c) Side-view structure. The blue, gray, and red balls are, respectively, the Ge atoms within the germanene layer, the Ag, and the Ge atoms of the Ag_2Ge surface alloy layer.

the optimized structures. Table S1 (in supplement material) gives the optimized spacing between the germanene layer and its underlying layer for different configurations. The closest calculated spacing to what we have measured experimentally (2.5 \AA in figure 3(b)) is 2.91 \AA which happens for the germanene layer on top of a bilayer Ag_2Ge in the bridge-Ag–Ag configuration.

Moreover, we calculated the germanene-substrate binding energy defined as $E_b = (E_{\text{tot}} - E_{\text{sub}} - E_{\text{ger}})/N_{\text{ger}}$ for all possible configurations (see table S2), with E_{tot} , E_{sub} , and E_{ger} being the total energy of the germanene/substrate system, that of the substrate, and that of the germanene layer, respectively. N_{ger} is the number of Ge atoms in the germanene layer. For the system of a germanene layer on a bilayer Ag_2Ge , the binding energy of the germanene-substrate and that of the Ag_2Ge layers with each other—i.e. the Ag_2Ge – Ag_2Ge binding energy—are lower than these binding energies for the other two structures (the germanene-on-monolayer- Ag_2Ge structure and germanene-on-trilayer- Ag_2Ge structure). Also, they can stably exist. Therefore, the germanene-on-bilayer Ag_2Ge bridge-Ag–Ag structure corresponds to our experiments.

4. Conclusion

In summary, we have studied the growth of germanium on Ag(111), and found the growth mode is crucially determined by the deposition rate. At low deposition rates, Ge atoms form irregular domains, whereas a layer of germanene forms when the deposition rate is three times higher. The V-shaped density of states and corresponding DFT calculations suggest that we are dealing with a germanene layer. This work is helpful to understand the controllable growth of germanene.

Authors' contributions

JD, GA, YY, XF and QW performed the STM experiments. PL did the DFT calculations. JD and LZ took part in preparing the manuscript with the input from all co-authors. AS provided many technical and text editorial suggestions. LZ and ZQ coordinated the research project. All authors participated in discussing the data.

Acknowledgments

This work is supported by the National Natural Science Foundation of China (Grant Nos. 51972106, 11904094 and 51772087), the Strategic Priority Research Program of Chinese Academy of Sciences (Grant No. XDB30000000), and Natural Science Foundation of Hunan Province, China (Nos. 2019JJ50034 and 2019JJ50073). P Li thanks China's Postdoctoral Science Foundation funded project (No. 2020M673364).

Data availability statement

The data generated and/or analysed during the current study are not publicly available for legal/ethical reasons but are available from the corresponding author on reasonable request.

ORCID iDs

Lijie Zhang  <https://orcid.org/0000-0001-8717-5724>

References

- [1] Novoselov K S, Geim A K, Morozov S V, Jiang D, Zhang Y, Dubonos S V, Grigorieva I V and Firsov A A 2004 Electric field effect in atomically thin carbon films *Science* **306** 666
- [2] Novoselov K S, Jiang D, Schedin F, Booth T J, Khotkevich V V, Morozov S V and Geim A K 2005 Two-dimensional atomic crystals *Proc. Natl Acad. Sci.* **102** 10451
- [3] Acun A *et al* 2015 Germanene: the germanium analogue of graphene *J. Phys.: Condens. Matter* **27** 443002
- [4] Qin Z 2017 Recent progress of graphene-like germanene *Acta Phys. Sin.* **66** 216802
- [5] Cahangirov S, Topsakal M, Akturk E, Sahin H and Ciraci S 2009 Two- and one-dimensional honeycomb structures of silicon and germanium *Phys. Rev. Lett.* **102** 236804
- [6] Li P, Cao J and Guo Z-X 2016 A new approach for fabricating germanene with Dirac electrons preserved: a first principles study *J. Mater. Chem. C* **4** 1736
- [7] Liu C C, Feng W X and Yao Y G 2011 Quantum spin Hall effect in silicene and two-dimensional germanium *Phys. Rev. Lett.* **107** 076802
- [8] Bampoulis P, Zhang L, Safaei A, van Gastel R, Poelsema B and Zandvliet H J W 2014 Germanene termination of Ge₂Pt crystals on Ge(110) *J. Phys.: Condens. Matter* **26** 442001
- [9] Dávila M E, Xian L, Cahangirov S, Rubio A and Le Lay G 2014 Germanene: a novel two-dimensional germanium allotrope akin to graphene and silicene *New J. Phys.* **16** 095002
- [10] Li L, Lu S-z, Pan J, Qin Z, Wang Y-q, Wang Y, Cao G-y, Du S and Gao H-J 2014 Buckled germanene formation on Pt(111) *Adv. Mater.* **26** 4820
- [11] Derivaz M, Dentel D, Stephan R, Hanf M-C, Mehdaoui A, Sonnet P and Pirri C 2015 Continuous germanene layer on Al(111) *Nano Lett.* **15** 2510
- [12] Zhang L, Bampoulis P, Rudenko A N, Yao Q, van Houselt A, Poelsema B, Katsnelson M I and Zandvliet H J W 2016 Structural and electronic properties of germanene on MoS₂ *Phys. Rev. Lett.* **116** 256804
- [13] Qin Z, Pan J, Lu S, Shao Y, Wang Y, Du S, Gao H-J and Cao G 2017 Direct evidence of Dirac signature in bilayer germanene islands on Cu(111) *Adv. Mater.* **29** 1606046
- [14] Jiao Z, Yao Q, Rudenko A N, Zhang L and Zandvliet H J W 2020 Germanium/MoS₂: competition between the growth of germanene and intercalation *Phys. Rev. B* **102** 205419
- [15] Li L and Zhao M 2013 First-principles identifications of superstructures of germanene on Ag(111) surface and h-BN substrate *Phys. Chem. Chem. Phys.* **15** 16853
- [16] Oughaddou H *et al* 2000 Ge/Ag(111) semiconductor-on-metal growth: formation of an Ag₂Ge surface alloy *Phys. Rev. B* **62** 16653
- [17] Liu Y, Zhuang J, Liu C, Wang J, Xu X, Li Z, Zhong J and Du Y 2017 Role of atomic interaction in electronic hybridization in two-dimensional Ag₂Ge nanosheets *J. Phys. Chem. C* **121** 16754
- [18] Lin C-H *et al* 2018 Single-layer dual germanene phases on Ag(111) *Phys. Rev. Mater.* **2** 024003
- [19] Zhuang J *et al* 2018 Dirac signature in germanene on semiconducting substrate *Adv. Sci.* **5** 1800207
- [20] Barkai M, Grünbaum E, Lereah Y and Deutscher G 1982 The epitaxial growth of germanium and silicon on an Ag(111) film on a mica substrate *Thin Solid Films* **90** 91
- [21] Zhang K, Bernard R, Borensztein Y, Cruguel H and Prévot G 2020 Growth of germanium–silver surface alloys followed by *in situ* scanning tunneling microscopy: absence of germanene formation *Phys. Rev. B* **102** 125418
- [22] Castro Neto A H, Guinea F, Peres N M R, Novoselov K S and Geim A K 2009 The electronic properties of graphene *Rev. Mod. Phys.* **81** 109
- [23] Zhang L, Bampoulis P, van Houselt A and Zandvliet H J W 2015 Two-dimensional Dirac signature of germanene *Appl. Phys. Lett.* **107** 111605
- [24] Kresse G and Joubert D 1999 From ultrasoft pseudopotentials to the projector augmented-wave method *Phys. Rev. B* **59** 1758
- [25] Kresse G and Hafner J 1993 *Ab initio* molecular dynamics for liquid metals *Phys. Rev. B* **47** 558
- [26] Perdew J P, Burke K and Ernzerhof M 1996 Generalized gradient approximation made simple *Phys. Rev. Lett.* **77** 3865
- [27] Feng B, Ding Z, Meng S, Yao Y, He X, Cheng P, Chen L and Wu K 2012 Evidence of silicene in honeycomb structures of silicon on Ag(111) *Nano Lett.* **12** 3507
- [28] Bernard R, Borensztein Y, Cruguel H, Lazzeri M and Prévot G 2015 Growth mechanism of silicene on Ag(111) determined by scanning tunneling microscopy measurements and *ab initio* calculations *Phys. Rev. B* **92** 045415
- [29] Liu X, Wei Z, Balla I, Mannix A J, Guisinger N P, Luijten E and Hersam M C 2017 Self-assembly of electronically abrupt borophene/organic lateral heterostructures *Sci. Adv.* **3** e1602356
- [30] Li J, Schneider W-D, Berndt R, Bryant O R and Crampin S 1998 Surface-state lifetime measured by scanning tunneling spectroscopy *Phys. Rev. Lett.* **81** 4464

- [31] Chang T-C, Hwang I-S and Tsong T T 1999 Direct observation of reaction-limited aggregation on semiconductor surfaces *Phys. Rev. Lett.* **83** 1191
- [32] Sun S *et al* 2020 Realization of a buckled antimonene monolayer on Ag(111) via surface engineering *J. Phys. Chem. Lett.* **11** 8976
- [33] Yuhara J, Fujii Y, Nishino K, Isobe N, Nakatake M, Xian L, Rubio A and Le Lay G 2018 Large area planar stanene epitaxially grown on Ag(111) *2D Mater.* **5** 025002
- [34] Wang Y, Li J, Xiong J, Pan Y, Ye M, Guo Y, Zhang H, Quhe R and Lu J 2016 Does the Dirac cone of germanene exist on metal substrates? *Phys. Chem. Chem. Phys.* **18** 19451
- [35] Yuhara J, Shimazu H, Ito K, Ohta A, Araidai M, Kurosawa M, Nakatake M and Le Lay G 2018 Germanene epitaxial growth by segregation through Ag(111) thin films on Ge(111) *ACS Nano* **12** 11632
- [36] Suzuki S *et al* 2020 Direct growth of germanene at interfaces between van der Waals materials and Ag(111) *Adv. Funct. Mater.* **31** 2007038